

Cite this: *J. Mater. Chem.*, 2011, **21**, 8987

www.rsc.org/materials

COMMUNICATION

A novel method for the synthesis of well-crystallized β -AlF₃ with high surface area derived from γ -Al₂O₃†

Wen-Zhi Jia, Ji-Qing Lu, Ping Chen, Yue-Juan Wang and Meng-Fei Luo*

Received 15th April 2011, Accepted 9th May 2011

DOI: 10.1039/c1jm11630d

Well-crystallized β -AlF₃ with high surface area was synthesized by a carbon template method. Porous γ -Al₂O₃ was filled with carbon and transformed into AlF₃ by fluorination. After removing the carbon template by thermal combustion, the resulting β -AlF₃ had a surface area of 114 m² g⁻¹. Temperatures for fluorination and thermal combustion were crucial for the phase composition of the resulting sample. The high surface area β -AlF₃ was very active for dismutation of CF₂Cl₂ due to its large amount of surface acid sites.

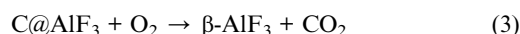
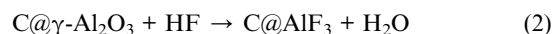
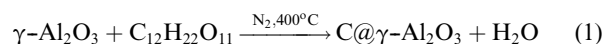
Aluminum fluoride (AlF₃) has many properties and applications such as electrolysis, electrical conductivity and fluoro-aluminate glasses. Moreover, AlF₃ is of great interest in heterogeneous catalysis as the well-known halogen exchange catalyst, which plays an important role in the synthesis of hydrofluorocarbons (HFCs) as Freon-alternatives and novel fluorinated organic compounds applied in pharmaceuticals.^{1,2}

AlF₃ could be synthesized through the fluorination of high surface area γ -Al₂O₃ with HF, NH₄F, SF₄, hydro-fluorocarbons, or chlorofluorocarbons.³ However, the resulting AlF₃ usually has a low surface area of 10–60 m² g⁻¹.

Recently, new methods have been developed to synthesize AlF₃ with high surface area, such as the NF₃ plasma-etching treatment of aluminum-rich zeolites reported by Delattre *et al.*,⁴ resulting in a surface area of 190 m² g⁻¹. Kemnitz *et al.*⁵ employed a sol-gel method to synthesize amorphous AlF₃ with a high surface area of 200 m² g⁻¹ (HS-AlF₃). Wolfgang *et al.*⁶ reported that Al₂O₃ reacting with HF solution and consecutive thermal decomposition resulted in β -AlF₃ with a surface area of 120 m² g⁻¹. However, by these methods, either the synthetic procedure is complicated or corrosive HF solution, explosive NF₃ and costly metal-alkoxide Al(O^{*i*}Pr)₃ are used. In particular, as halogen exchange reactions usually take place in a temperature range of 200 to 400 °C,⁷ amorphous AlF₃ may undergo phase transition under rigorous reaction conditions. Therefore, well crystallized AlF₃ is more thermally stable, and thus desirable for catalysis purpose.

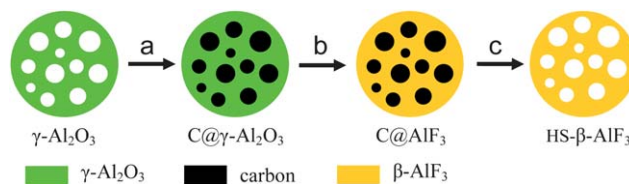
In spite of AlF₃ existing in crystalline forms of α , β , η , θ , κ ,⁸ the β -phase possesses significant catalytic activity for halogen exchange and strong Lewis acid sites⁹ compared to the α -phase. For heterogeneous Cl/F exchange reaction, catalysts with strong Lewis acid sites are required.^{1,10} More importantly, the reactivity is generally correlated to the amount of surface acid sites on the AlF₃, and thus high surface area AlF₃ is more advantageous in the reactions.

In this work, we report a novel method for converting γ -Al₂O₃ to high surface area β -AlF₃ (hereafter denoted as HS- β -AlF₃) by the gas-solid fluorination reaction with gaseous HF. The preparation process could be described as the following equations:



Firstly, solid γ -Al₂O₃ was immersed in an aqueous sucrose (C₁₂H₂₂O₁₁) solution and the dried mixture was thermally treated under N₂ flow at 400 °C to obtain a γ -Al₂O₃ with carbon filled in the pores (denoted as C@ γ -Al₂O₃), as shown in eqn (1). Then the C@ γ -Al₂O₃ was fluorinated with gaseous HF at 250 °C to obtain C@AlF₃ [eqn (2)]. Finally, the carbon template was removed by combustion under oxygen flow to obtain well crystalline β -AlF₃ [eqn (3)]. The process is demonstrated in Scheme 1.

Fig. 1 shows the N₂ adsorption-desorption isotherms and XRD patterns of the samples during the preparation procedure. From Fig. 1a, it can be seen that after carbon filling into the pores of γ -Al₂O₃, the surface area of γ -Al₂O₃ dramatically declines from 347 to 77 m² g⁻¹, due to the blocking of pores by carbon particles. The C@AlF₃ has similar surface area to the C@Al₂O₃, indicating the



Scheme 1 Schematic diagram for the synthesis of HS- β -AlF₃. a: filling carbon hard template; b: fluorination with gaseous HF; c: combustion of carbon template in oxygen atmosphere.

Zhejiang Key Laboratory for Reactive Chemistry on Solid Surfaces
Institute of Physical Chemistry Zhejiang Normal University, Jinhua,
China. E-mail: mengfeiluo@zjnu.cn; Fax: (+86) 579-82282595; Tel:
(+86) 579-82283910

† Electronic supplementary information (ESI) available: Details of experimental procedures, tables, Raman, SEM-EDX, TG-DTA, FTIR and graphics. See DOI: 10.1039/c1jm11630d

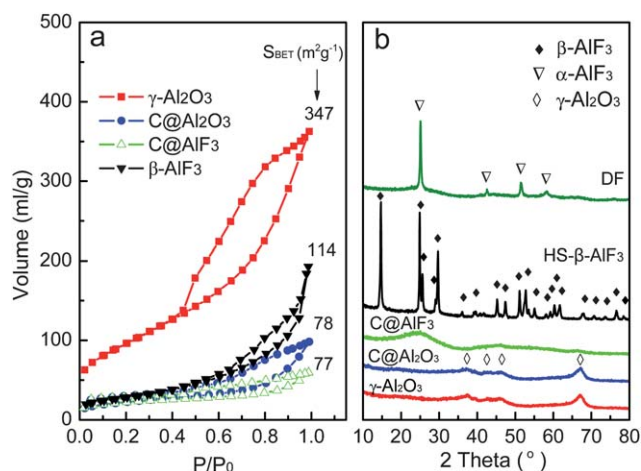


Fig. 1 a) N_2 adsorption-desorption isotherms, BET areas and b) XRD patterns of samples represented in the synthesis procedure. DF means the direct fluorination of $\gamma\text{-Al}_2\text{O}_3$ with HF.

maintenance of the sample structure. When the carbon template is removed, the resulting HS- $\beta\text{-AlF}_3$ has a surface area of $114 \text{ m}^2 \text{ g}^{-1}$. Also, as can be seen from Fig. 1b, the $\gamma\text{-Al}_2\text{O}_3$ crystallite phase remains unchanged after filling of carbon template ($\text{C@Al}_2\text{O}_3$). After fluorination, the sample is amorphous (C@AlF_3). When the carbon is removed under a thermal treatment in oxygen at 425°C for 8 h, well crystallized HS- $\beta\text{-AlF}_3$ is obtained, which exhibits the hexagonal tungsten bronze type structure.^{8,11} This implies that during the thermal treatment, amorphous AlF_3 formed in fluorination stage transforms to $\beta\text{-AlF}_3$. However, direct fluorination of $\gamma\text{-Al}_2\text{O}_3$ at 250°C results in the formation of $\alpha\text{-AlF}_3$, which has a surface area of only $15 \text{ m}^2 \text{ g}^{-1}$.

In order to further describe the preparation process for HS- $\beta\text{-AlF}_3$, Raman spectroscopy was also conducted and the results are shown in the ESI (Fig. S1†). Concerning the strong fluorescence and the fact that $\gamma\text{-Al}_2\text{O}_3$ and AlF_3 has no visible Raman signals, the Raman spectra are not very informative. However, distinct bands at 1360 and 1600 cm^{-1} which are characteristic of carbon¹² are found in the spectra for $\text{C@Al}_2\text{O}_3$ and C@AlF_3 . This confirms that carbon is present in $\gamma\text{-Al}_2\text{O}_3$, which is in agreement with the N_2 adsorption-desorption isotherms in Fig. 1a.

Fig. 2 shows the representative SEM and TEM images of the HS- $\beta\text{-AlF}_3$ sample fluorinated at 250°C . As can be seen in Fig. 2a, the synthesized material is disordered and flocculated. Also, EDX analysis of the selected area (Fig. S2†) shows that the sample contains

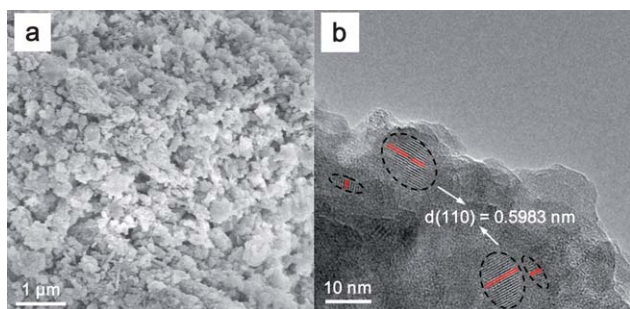


Fig. 2 a) SEM and b) TEM images of synthesized HS- $\beta\text{-AlF}_3$.

25.08% Al and 74.92% F, which is very close to an Al/F ratio of 3, indicating that the Al_2O_3 is completely fluorinated to form AlF_3 . The TEM image (Fig. 2b) also shows the interplane distance of the $\beta\text{-AlF}_3$ (110) crystal face (0.5983 nm), which further confirms the formation of $\beta\text{-AlF}_3$.

Since the fluorination process is crucial for the resulting AlF_3 , the effect of fluorination temperature on the final phase composition of the sample has been investigated. As can be seen in Fig. 3a, the $\text{C@Al}_2\text{O}_3$ cannot be completely fluorinated at 200°C as the diffraction peaks of $\gamma\text{-Al}_2\text{O}_3$ are still present in the pattern. When the fluorination temperature is higher than 275°C , however, diffraction peaks due to $\alpha\text{-AlF}_3$ appear. Fig. 3b shows the XRD patterns of the template-removed samples with different fluorination temperatures. It can be seen that the $\text{C@Al}_2\text{O}_3$ cannot be completely fluorinated at 200°C because the weak diffraction peaks of $\gamma\text{-Al}_2\text{O}_3$ remain. When fluorinated at 250°C , only diffraction peaks due to $\beta\text{-AlF}_3$ are observed, implying the complete fluorination of $\gamma\text{-Al}_2\text{O}_3$ to $\beta\text{-AlF}_3$. When the fluorination temperature is higher than 250°C , it is found that the peak intensity at 14.8° assigned to $\beta\text{-AlF}_3$ (110) plane decreases while that at 24.9° assigned to (002) plane of $\beta\text{-AlF}_3$ and (100) plane of $\alpha\text{-AlF}_3$ significantly increases, suggesting the formation of $\alpha\text{-AlF}_3$. Therefore, the fluorination temperature of 250°C seems appropriate for the formation of $\beta\text{-AlF}_3$.

Table 1 summarizes the phase composition, average crystallite size, F/Al ratio and surface area of the samples fluorinated at different temperatures, determined by XRD, EDX and BET techniques, respectively. When the fluorination temperature is low (200°C), the sample contains unfluorinated $\gamma\text{-Al}_2\text{O}_3$, which is also confirmed by EDX analysis which shows that the F/Al ratio is 1.92. At high fluorination temperature ($\geq 250^\circ\text{C}$), the sample is completely transformed to AlF_3 , as the F/Al ratio is very close to 3 : 1. However, the content of $\alpha\text{-AlF}_3$ in the sample increases with increasing temperature, and the sample fluorinated at 350°C contains only $\alpha\text{-AlF}_3$.

As for the surface area, it can be seen that it declines dramatically with increasing fluorination temperature. This is due to the fact that $\gamma\text{-Al}_2\text{O}_3$ could be readily fluorinated to form thermostable $\alpha\text{-AlF}_3$ at high temperature because of their high lattice energies,^{5,9} and the crystallite size gradually increases with fluorination temperature, which results in the decline of surface area. On the other hand, the decline in surface area implies that some pore structure may be destroyed during high temperature fluorination.

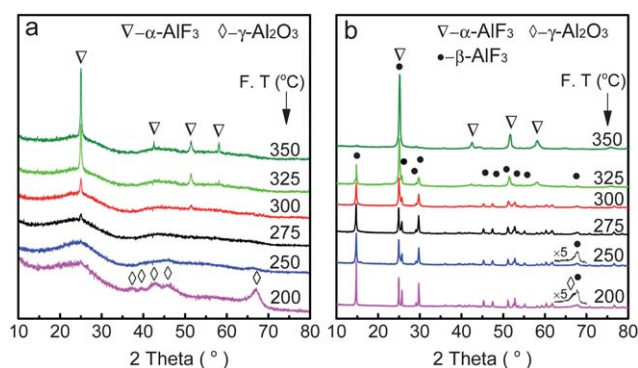


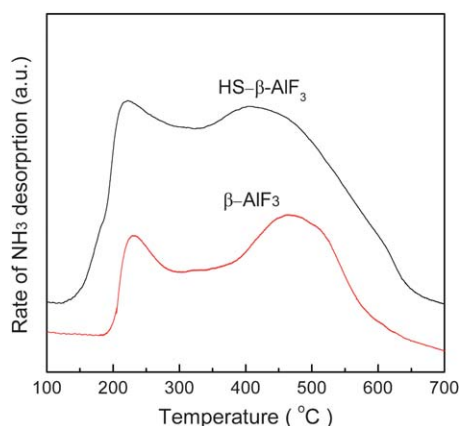
Fig. 3 XRD patterns of samples with different fluorination temperatures. a) fluorination process of $\text{C@Al}_2\text{O}_3$; b) samples after removal of carbon template. FT means the fluorination temperature.

Table 1 Properties of samples with different fluorination temperatures

Fluorination $T/^{\circ}\text{C}$	Phase composition (wt%)	Average crystallite size/nm	F/Al molar ratio	Surface area/ $\text{m}^2 \text{g}^{-1}$
200	$\beta\text{-AlF}_3$	77.2	1.92 : 1	136
	$\gamma\text{-Al}_2\text{O}_3$	n.d		
250	$\beta\text{-AlF}_3$ (100)	48.5	2.98 : 1	114
275	$\beta\text{-AlF}_3$ (96.3)	41.0	2.99 : 1	85
	$\alpha\text{-AlF}_3$ (3.7)	10.0		
300	$\beta\text{-AlF}_3$ (85.2)	33.5	3.02 : 1	72
	$\alpha\text{-AlF}_3$ (14.8)	15.1		
325	$\beta\text{-AlF}_3$ (58.1)	18.4	3.01 : 1	65
	$\alpha\text{-AlF}_3$ (41.9)	22.3		
350	$\alpha\text{-AlF}_3$ (100)	31.2	2.99 : 1	22

It was reported that amorphous AlF_3 could be transformed to $\beta\text{-AlF}_3$ at 350–475 $^{\circ}\text{C}$, while the transformation of $\beta\text{-AlF}_3$ to $\alpha\text{-AlF}_3$ will take place in the temperature range of 475–650 $^{\circ}\text{C}$.¹³ Therefore, the choice of the temperature for removal of carbon template in the present synthesis is essential to obtain the desired $\beta\text{-AlF}_3$. It should be noted that the complete combustion of carbon requires a temperature of 500 $^{\circ}\text{C}$ confirmed in our experiment, at which the resulting sample is $\alpha\text{-AlF}_3$. By the addition of KNO_3 in the C@AlF_3 , the carbon template could be efficiently combusted at 425 $^{\circ}\text{C}$. The promoting effect of KNO_3 in soot combustion has been widely reported.¹⁴ Also, our TG-DTA experiment shows that the addition of KNO_3 has lowered the carbon combustion temperature by 50 $^{\circ}\text{C}$ (Fig. S3†) compared to that without KNO_3 . The lowered combustion temperature could effectively inhibit the phase transformation of $\beta\text{-AlF}_3$, which is also a key factor in obtaining the HS- $\beta\text{-AlF}_3$.

The acidic properties of the prepared HS- $\beta\text{-AlF}_3$ have been characterized by FTIR spectroscopy of pyridine adsorption and NH_3 -temperature programmed desorption (NH_3 -TPD), and more importantly by its catalytic properties. After pyridine adsorption, the FTIR spectrum (Fig. S4†) of the HS- $\beta\text{-AlF}_3$ shows intense bands at 1454 and 1632 cm^{-1} , which indicates Lewis acid sites.¹⁵ The NH_3 -TPD profile of HS- $\beta\text{-AlF}_3$ is shown in Fig. 4. It shows two distinct desorption peaks at about 220 and 460 $^{\circ}\text{C}$. The amount of surface acidic sites of the HS- $\beta\text{-AlF}_3$ is calculated to be 876 $\mu\text{mol g}^{-1}_{\text{cat}}$. This is among the highest values reported in the literature (Table S1†). For comparison, a conventional $\beta\text{-AlF}_3$ prepared by thermal treating

**Fig. 4** NH_3 -TPD profiles of $\beta\text{-AlF}_3$ samples.**Table 2** Dismutation of CF_2Cl_2 over AlF_3 catalysts

Sample	Surface area/ $\text{m}^2 \text{g}^{-1}$	CF_2Cl_2 conversion (%)			
		300 $^{\circ}\text{C}$	250 $^{\circ}\text{C}$	200 $^{\circ}\text{C}$	150 $^{\circ}\text{C}$
$\alpha\text{-AlF}_3$	15	54	16	10	2
$\beta\text{-AlF}_3$	41	89	78	25	11
HS- $\beta\text{-AlF}_3$	114	95	85	52	31

$\text{AlF}_3 \cdot 3\text{H}_2\text{O}$ according to ref. 16 resulted in a surface area of 41 $\text{m}^2 \text{g}^{-1}$ and surface acidic sites of 421 $\mu\text{mol g}^{-1}_{\text{cat}}$.

The HS- $\beta\text{-AlF}_3$ has also been tested for catalytic CCl_2F_2 dismutation [eqn (4)].



Table 2 lists the catalytic activity of various AlF_3 samples for the reaction. It can be seen that the HS- $\beta\text{-AlF}_3$ is much more active than the $\alpha\text{-AlF}_3$ and low surface area $\beta\text{-AlF}_3$ at low reaction temperature, which is due to the higher amount of surface acidic sites. In addition, the synthesized HS- $\beta\text{-AlF}_3$ shows good stability during the reaction, with 95% conversion of CF_2Cl_2 in a reaction period of 10 h at 300 $^{\circ}\text{C}$ (Fig. S5†). A comparison of the fresh and the used samples by XRD revealed that there is no phase transition during the reaction (Fig. S6†). Also, the used catalyst has a surface area of 108 $\text{m}^2 \text{g}^{-1}$, suggesting that the catalyst structure remains unchanged.

To summarize, well crystallized HS- $\beta\text{-AlF}_3$ is prepared by a solid-template method, derived from the fluorination of carbon filled $\gamma\text{-Al}_2\text{O}_3$ and thermal removal of the carbon template. The resulting HS- $\beta\text{-AlF}_3$ has large amount of surface acidic sites due to its high surface area, which is beneficial for halogen exchange reaction such as dismutation of CF_2Cl_2 or CHFCl_2 . The synthesized HS- $\beta\text{-AlF}_3$ is thermally stable, which could be applied to high temperature reactions. More importantly, other metal fluorides with high surface area such as MgF_2 may also be prepared in a similar way.

Acknowledgements

This work is financially supported by the National Science Foundation of China (Grant No. 20873125) and the Natural Science Foundation of Zhejiang Province (Grant No. 2009C31050). And also we thank Prof. Dr Fengshou Xiao (Zhejiang University, China) for the valuable discussion.

Notes and references

- O. Boese, E. S. Wolfgang and E. Kemnitz, *et al.*, *Phys. Chem. Chem. Phys.*, 2002, **4**, 2824; H. D. Quan, H. Yang and A. Sekiya, *J. Fluorine Chem.*, 2004, **125**, 1169.
- T. Skapin, G. Tavčar and A. Benčan, *et al.*, *J. Fluorine Chem.*, 2009, **130**, 1086.
- A. Hess and E. Kemnitz, *J. Catal.*, 1994, **149**, 449; R. I. Hedge and M. A. Barteau, *J. Catal.*, 1989, **120**, 387; P. J. Chupas, M. F. Ciruolo and C. P. Grey, *et al.*, *J. Am. Chem. Soc.*, 2001, **123**, 1694.
- J. L. Delattre, P. J. Chupas and A. M. Stacy, *et al.*, *J. Am. Chem. Soc.*, 2001, **123**, 5364.
- E. Kemnitz, U. Groß and S. Rüdiger, *et al.*, *Angew. Chem., Int. Ed.*, 2003, **42**, 4251; S. K. Ruediger, U. Groß and E. Kemnitz, *et al.*, *J. Mater. Chem.*, 2005, **15**, 588.
- K. Wolfgang, C. Haesner and K. Köhler, *et al.*, *Inorg. Chim. Acta*, 2006, **359**, 4851.
- E. Ünveren, E. Kemnitz and W. E. S. Unger, *et al.*, *J. Phys. Chem. B*, 2005, **109**, 1903; J. He, G. Q. Xie and M. F. Luo, *et al.*, *J. Catal.*, 2008, **253**, 1.
- R. König, W. E. S. Unger and E. Kemnitz, *et al.*, *J. Fluorine Chem.*, 2010, **131**, 91.
- H. Bozorgzadeh, E. Kemnitz and J. M. Winfield, *et al.*, *J. Fluorine Chem.*, 2001, **107**, 45.
- C. G. Krespan and D. A. Dixon, *J. Fluorine Chem.*, 1996, **77**, 117.
- A. La Bail, C. Jacobni and J. L. Fourquet, *et al.*, *J. Solid State Chem.*, 1988, **77**, 96; A. Pawlik, R. König and E. Kemnitz, *et al.*, *J. Phys. Chem. C*, 2009, **113**, 16674.
- R. Escibano, J. J. Sloan and T. Dudev, *et al.*, *Vib. Spectrosc.*, 2001, **26**, 179.
- C. Alonso, A. Morato and J. E. Sueiras, *et al.*, *Chem. Mater.*, 2000, **12**, 1148.
- P. Fang, J. Q. Lu and M. F. Luo, *et al.*, *Acta Phys. Chim. Sin.*, 2007, **23**, 1275.
- G. Eltanany, S. Rüdiger and E. Kemnitz, *et al.*, *J. Mater. Chem.*, 2008, **18**, 2268; G. Busca, *Catal. Today*, 1996, **27**, 323; J. M. Winfield, *J. Fluorine Chem.*, 2009, **130**, 1069.
- T. Krah, R. Stösser and E. Kemnitz, *et al.*, *Inorg. Chem.*, 2003, **42**, 6474.